Monthly Notices of the ROYAL ASTRONOMICAL SOCIETY

MNRAS **524,** L89–L93 (2023) https://doi.org/10.1093/mnrasl/slad081
Advance Access publication 2023 June 22

Microquasar Cyg X-3 – a unique jet-wind neutrino factory?

Karri I. I. Koljonen [1,2,3★] Konstancja Satalecka,[2] Elina J. Lindfors[2] and Ioannis Liodakis [2]

[1]*Institutt for Fysikk, Norwegian University of Science and Technology, Høgskloreringen 5, Trondheim 7491, Norway*
[2]*Finnish Centre for Astronomy with ESO (FINCA), University of Turku, Väisäläntie 20, FI-21500 Piikkiö, Finland*
[3]*Aalto University, Metsähovi Radio Observatory, PO Box 13000, FI-00076 Aalto, Finland*

Accepted 2023 June 16. Received 2023 May 31; in original form 2023 February 17

ABSTRACT

The origin of astrophysical neutrinos is one of the most debated topics today. Perhaps the most robust evidence of neutrino counterpart comes from supermassive black holes in active galactic nuclei associated with strongly collimated outflows, or jets, that can accelerate particles to relativistic energies and produce neutrinos through hadronic interactions. Similar outflows can also be found from X-ray binaries, or 'microquasars', that consist of a neutron star or a stellar-mass black hole accreting matter from a non-degenerate companion star. In some cases, these systems can accelerate particles up to GeV energies implying an efficient acceleration mechanism in their jets. Neutrino production in microquasar jets can be expected with suitable conditions and a hadronic particle population. Microquasar Cyg X-3 is a unique, short orbital period X-ray binary hosting a Wolf–Rayet companion star with a strong stellar wind. The interaction of the dense stellar wind with a relativistic jet leads to particle collisions followed by high-energy gamma-ray and potentially neutrino emission. Here, using the 10-yr neutrino candidate sample of the IceCube neutrino observatory, we find that the events with the highest spatial association with Cyg X-3 occur during short-lived high-energy gamma-ray flaring periods indicating the possible astrophysical nature of these events.

Key words: neutrinos – binaries: close – stars: individual: Cyg X-3 – stars:jets – stars: winds, outflows – X-rays: binaries.

1 INTRODUCTION

Cyg X-3 is a unique X-ray binary (XRB; Giacconi et al. 1967), consisting (most likely) of a black hole and a Wolf–Rayet companion star (van Kerkwijk et al. 1992; Koljonen & Maccarone 2017) – the only known such system in our Galaxy (Lommen et al. 2005). The Wolf–Rayet companion is an evolved massive star with a strong stellar wind. The short 4.8-h orbit (Parsignault et al. 1972) exposes the compact object to the dense wind, causing many peculiar properties (Koljonen et al. 2018), including high-energy (HE; >100 MeV) gamma-ray emission (Fermi LAT Collaboration 2009; Tavani et al. 2009) observed during a specific phase of an outburst event (Koljonen et al. 2010).

XRBs undergo bright outburst periods that are thought to arise from a change in the rate at which matter flows from the companion star to the accretion disc. Jets in XRBs are continuously launched during the 'hard' X-ray state when the X-ray emission is dominated by a hot population of electrons, typically denoted as the 'corona', and are quenched in the 'soft' state that is dominated by the relatively cooler emission from the accretion disc. As the system transitions from the hard to the soft state, the steady jet switches off, and a transient jet is launched, characterized by rapidly varying optically thin radio emission from blobs or shocks of plasma launched in the outflow (e.g. Fender et al. 1999; Fender, Belloni & Gallo 2004).

The HE gamma-ray emission requires an efficient mechanism for producing relativistic particles that naturally occur in a jet. However, only a few XRBs have been seen in GeV energies. In Cyg X-3, the HE gamma-ray emission is sporadic, typically associated with the transition to/from the soft state (Koljonen et al. 2010, 2018), or occasionally during minor flaring episodes in the soft state (Fermi LAT Collaboration 2009; Tavani et al. 2009; Bulgarelli et al. 2012; Corbel et al. 2012). These correspond to times when the jet is either shutting down, i.e. the system is transitioning to the soft state with quenched jet and coronal emission, or the jet is beginning to form. The HE gamma-ray emission is also orbitally modulated, placing the emitting region relatively close to the compact object (Fermi LAT Collaboration 2009). The maximum flux occurs when the compact object is behind the companion star, where the optical depth in the line of sight through the companion stellar wind is the largest. This has provoked scenarios where the HE gamma-rays are produced by the interaction between the jet and the stellar wind either by leptonic (inverse-Compton scattering of stellar photons by the relativistic electrons in the jet; Dubus, Cerutti & Henri 2010; Piano et al. 2012; Zdziarski et al. 2012) or hadronic processes (Romero et al. 2003; Piano et al. 2012; Sahakyan, Piano & Tavani 2014).

In the hadronic scenario, the jet is populated with protons that collide with the protons/photons of the stellar wind. These collisions produce pions and, subsequently, gamma-rays from pion decay products that can reach very high energies (VHEs; >100 GeV). This mechanism also produces neutrinos, which makes Cyg X-3 an attractive neutrino candidate (IceCube Collaboration 2013). So far, Cyg X-3 has not been observed in VHE gamma-rays (Aleksić et al. 2010; Archambault et al. 2013). This could be explained by the close proximity of the emitting region to the compact object and the VHE gamma-rays having a stronger absorption probability than the lower energy ones (Sahakyan et al. 2014). Nevertheless, if hadronic

★ E-mail: karri.koljonen@ntnu.no

processes produce these gamma-rays, the accompanying neutrino emission would be able to escape.

In a recent work, a neutrino signal was searched from XRBs, including Cyg X-3 (Abbasi et al. 2022). Using the 10-yr data base of neutrino events by the IceCube Observatory, they found that Cyg X-3 was the most significant source in their time-integrated search (pre- and post-trial p-values of 0.009 and 0.036, respectively). The energies of the associated events did not surpass 5 TeV, therefore, the expected neutrino event energies are low. This makes it difficult to separate the possible astrophysical neutrino candidates from background events that dominate the low energies.

A way to suppress the background events is to use time-dependent analysis by concentrating on the times of XRB outbursts often accompanied by increased jet emission in the hard state, which would be the most likely phase of neutrino emission. Abbasi et al. (2022) used hard X-ray monitoring data to separate XRB outbursts from persistent/quiescent emission to increase the likelihood of the signal. However, this analysis produced a less significant signal than the time-integrated one for Cyg X-3. What sets Cyg X-3 apart from most XRBs is the unusual companion star and the short orbital period that places the jet in a dense field of stellar wind particles. Koljonen et al. (2018) suggested a scenario where the jet constantly evacuates a cocoon in the stellar wind during the hard state, moving the work surface further out to a less dense environment. In contrast, in the soft state, the jet switches off, allowing the wind to refill the cocoon and providing a work surface for the newly forming jet in a much denser region when the source returns to the hard state or produces transient jet ejecta. These transitional phases are the times when we observe the HE gamma-ray emission (Fermi LAT Collaboration 2009; Tavani et al. 2009; Bulgarelli et al. 2012; Corbel et al. 2012; Piano et al. 2012). Therefore, these times also enhance the probability of observing neutrinos with the increased rate of jet and stellar wind particle collisions.

Considering the above, in this letter, we performed a time-dependent search during the high states of HE gamma-ray emission in Cyg X-3. We show tantalizing evidence that the HE gamma-ray emitting periods might also be periods of neutrino emission.

2 OBSERVATIONS

We utilized the IceCube Observatory (Aartsen et al. 2017) 10-yr event sample that contains track-like neutrino candidates detected between April 2008 and July 2018 (IceCube Collaboration 2021). The track-like signal events arise primarily from the interactions of muon neutrinos that mainly originate from cosmic rays interacting with the atmosphere but with a small fraction also from astrophysical sources. Based on the track orientation and the deposited energy, a proxy for the neutrino energy and the origin in the sky can be estimated. Details of the event selection process can be found in Abbasi et al. (2022). The 10-yr sample assumes a lower limit on the estimated angular uncertainty of 0.2 deg.

In addition, we used X-ray monitoring data from *Swift*/BAT (Krimm et al. 2013) and obtained the daily averaged 15–50 keV fluxes from their web interface, and weekly averaged 0.1–100 GeV *Fermi*-LAT detections (TS $>$ 4) of Cyg X-3 from the *Fermi*-LAT light-curve repository (Abdollahi et al. 2023).

3 RESULTS

To associate an IceCube track event with Cyg X-3, we make use of the spatial probability function and the expected time profile of the neutrino emission. The spatial probability function is constructed by

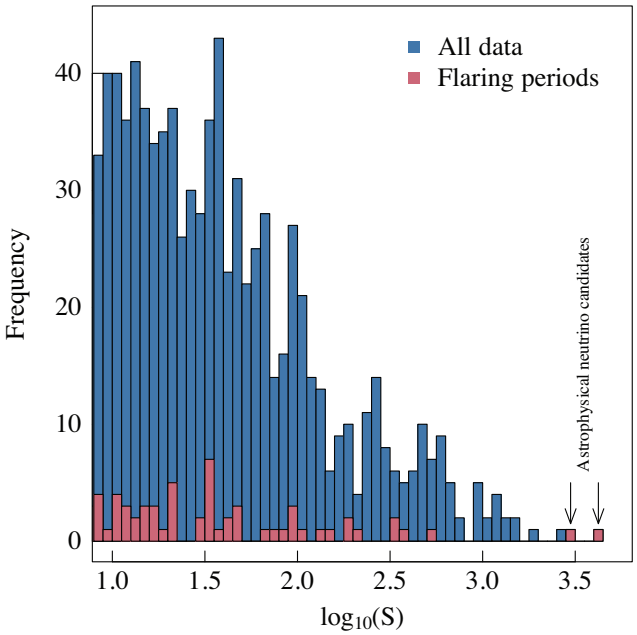

Figure 1. The spatial probability density distribution of all IceCube track-like neutrino events in the ±5 deg band around Cyg X-3. The events occurring during the HE gamma-ray flaring periods are highlighted in red. The two astrophysical neutrino candidates are marked with arrows.

calculating two-dimensional Gaussians in the sky with the widths based on the reconstructed angular resolution (σ_i) and the centroids based on the reconstructed position (x_i) of each event and recording their value at the location of the target (x_s)

$$S_i(x_i, x_s, \sigma_i) = \frac{1}{2\pi\sigma_i^2}\exp\Big(-\frac{(x_i - x_s)^2}{2\sigma_i^2}\Big). \quad (1)$$

Fig. 1 shows the values of the spatial probability density distributions at the location of Cyg X-3 of all IceCube track-like neutrino events and those during the HE gamma-ray flaring periods highlighted in blue and red, respectively, in the ±5 deg band around Cyg X-3 declination. The same values are plotted in Fig. 2 (bottom panel) together with the hard X-ray (top panel) and the HE gamma-ray (middle panel) monitoring observations. The HE gamma-ray flaring epochs (marked as grey vertical bars in Fig. 2) occur in periods of low hard X-ray emission. The two events having the strongest spatial association to Cyg X-3 (encircled points in Fig. 2 and arrows in Fig. 1) occurred during HE gamma-ray flaring periods at the beginning of 2011 and 2016, making them intriguing candidates for astrophysical neutrinos (their properties are tabulated in Table 1).

In addition, we consider two time probability functions of the expected neutrino emission. First, a top-hat profile, where the time profile is set to $T_i(t_i, \sigma_w) = 1/\sigma_w$, for all events with t_i inside the HE gamma-ray emission time interval (as shown in Fig. 2, grey bands), and otherwise zero. Here, σ_w is the width of a given HE gamma-ray emission time interval. Secondly, a Gaussian profile, where the time profile is set to

$$T_i(t_i, T_0, \sigma_w) = \frac{1}{\sqrt{(\pi/2)}\sigma_w}\exp\Big(-\frac{2(t_i - T_0)^2}{\sigma_w^2}\Big), \quad (2)$$

where T_0 is the mid-point of a given HE gamma-ray emission time interval, and the width of the Gaussian profile is considered as half of the HE gamma-ray emission time interval σ_w. In addition, we apply an additional weighting by the orbital phase, where the maximum

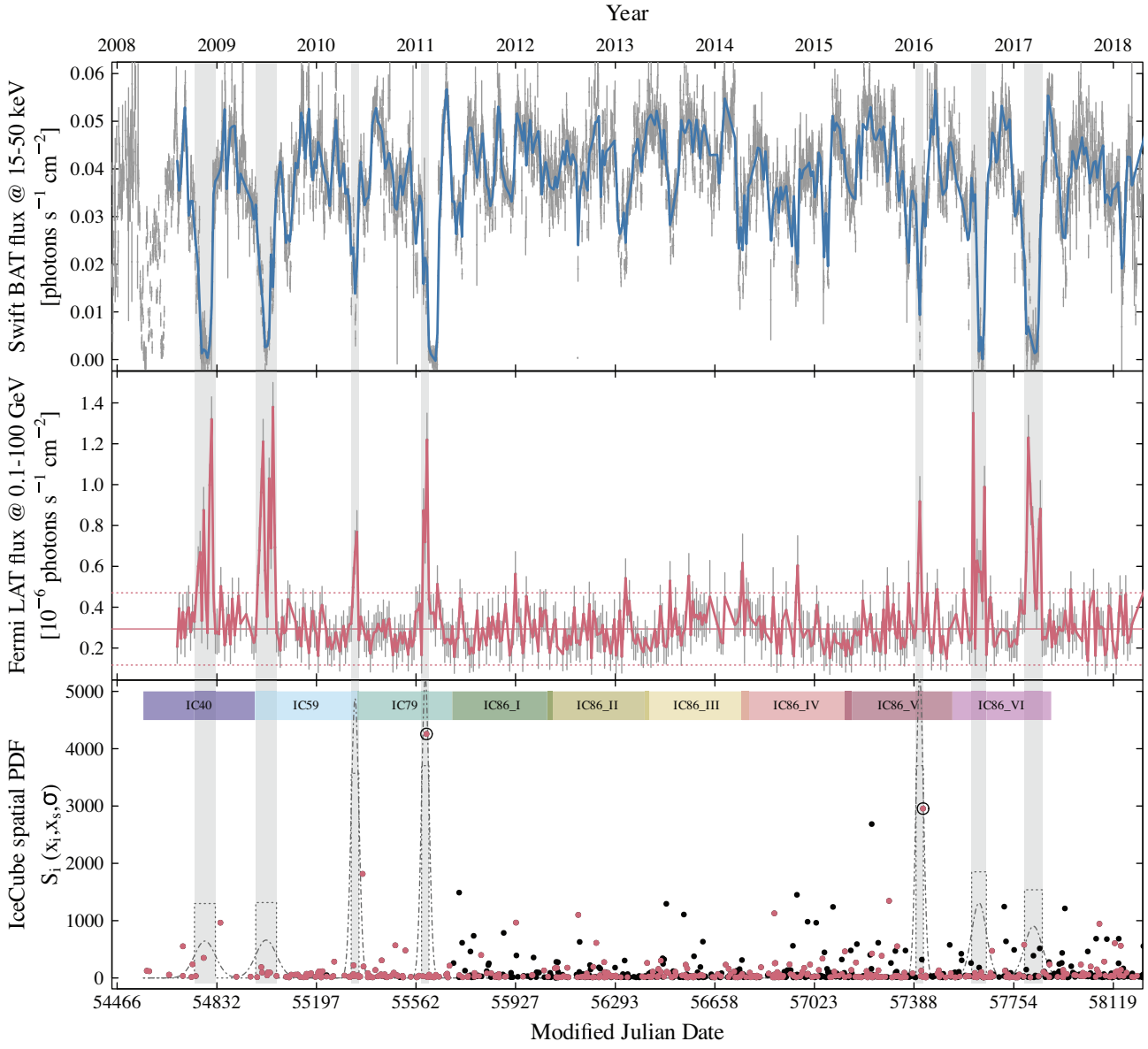

Figure 2. *Top:* Daily *Swift*/BAT 15–50 keV hard X-ray monitoring data of Cyg X-3 with a weekly average overplotted as a solid blue line. The 1σ error bars of the daily measurement are shown in grey. *Middle:* Weekly averaged 0.1–100 GeV *Fermi*-LAT monitoring data (TS $>$ 4) of Cyg X-3. HE gamma-ray flaring epochs are marked as grey areas and expanded to cover all panels. A horizontal solid line marks the average HE gamma-ray flux level outside the flaring epochs, with two standard deviations of the low-level data marked as dashed lines around the mean. The 1σ error bars of the weekly measurements are shown in grey. *Bottom:* Non-normalized spatial probability densities of IceCube events from a 10-deg band around Cyg X-3 declination. For clarity, we plot only those events with $S > 10$. The events with energies higher than 1 TeV are marked in red. The astrophysical neutrino event candidates are encircled. We also plot the shapes of the top-hat (dotted lines) and Gaussian (dot–dashed lines) time probability functions.

Table 1. The astrophysical neutrino candidate properties from Cyg X-3.

Event time (MJD)	RA (deg)	Dec. (deg)	Muon energy (TeV)	Ang. res. (deg)	Phase[a]
55600.51099	308.127	40.973	2.09	0.35	0.8
57421.23851	308.478	41.066	3.31	0.35	0.4

[a]Orbital phase calculated using epheremis from Antokhin & Cherepashchuk (2019).

weight (1) is given for orbital phases close to the superior conjuction, and the minimum weight (0.5) close to the inferior conjuction to mimic the effect of the observed high-energy gamma-ray orbital modulation (Fermi LAT Collaboration 2009; Zdziarski et al. 2018; Prokhorov & Moraghan 2022). The total signal probability function is then a product of the spatial and time probability functions weighted according to the orbital phase.

To estimate the chance coincidence probability of these events being just background, we performed 'pseudo-experiments' using the experimental data itself. Due to the azimuthal symmetry of IceCube and a large number of background events in the data, it is possible to take a declination band around the target's declination (here, we used $\pm$5 deg) and scramble the azimuthal components of all events in this band to give a realistic and pure background simulation.

We simulated the background for every season separately as they have different systematic effects. The scrambling was done 10^5 times,

and in each case, we calculated the total signal probability density of each event at the target location and recorded the event time using the two time profiles mentioned above and orbital phase weighting. These were then compared to the total signal probability densities of the actual data during the HE gamma-ray flaring windows.

The fraction of background simulations with one event having an equal or greater total signal probability density at the location of Cyg X-3 in any HE gamma-ray flaring period as the neutrino candidate with the highest probability of association is 0.9 per cent (2.6σ) using the Gaussian time profile for the flares. Similarly, The fraction of background simulations with two events having an equal or greater total signal probability densities as observed in any HE gamma-ray flaring period is 0.09 per cent (3.3σ). Similar values were obtained with the top-hat time profile.

In addition, we used PSLAB,[1] an open source code package to perform IceCube point source analyses. Using this package, we performed time-dependent point source analysis using the top-hat time profile according to the HE gamma-ray flaring windows determined above. In this analysis, the energy of the muon event is also taken into account (assuming a fixed $\Gamma = -2.4$ spectrum). The best-fitting number of signal events in this analysis is 2.6. The probability of this signal being background is 5.5 per cent (1.9σ). The lower probability of association as compared to the above likely arises from the soft spectrum as the bulk of the signal arises at the low, background-like energies.

4 DISCUSSION

4.1 Comparison with the expected number of neutrinos from Cyg X-3

To estimate the expected neutrino flux emitted during the HE gamma-ray flaring periods, we assume that the gamma-rays and neutrinos are produced in proton–proton collisions. This assumption is not necessarily true as a part or all the observed gamma-rays can arise from leptonic processes (Dubus et al. 2010; Piano et al. 2012; Zdziarski et al. 2018). We use the model of Sahakyan et al. (2014) that is based on the proton–proton collision process analytical estimates from Kelner, Aharonian & Bugayov (2006) and assume a power-law distributed proton with an index of $\Gamma = -2.4$ and a high-energy cut-off at 100 TeV. This value is motivated by the expected cut-off in the cosmic ray energies from Galactic sources. We do not consider the proton–photon collisions here as the estimated neutrino flux at 1 TeV is two-to-three orders of magnitude smaller than in the proton–proton case (Baerwald & Guetta 2013; Abbasi et al. 2022). The unabsorbed HE gamma-ray fluxes range from $\sim 2 \times 10^{-12}$ erg s^{-1} cm^{-2} at 1 TeV down to $\sim 5 \times 10^{-13}$ erg s^{-1} cm^{-2} at 50 TeV. We then converted the HE gamma-ray fluxes at 1–50 TeV to neutrino fluxes using the fact that the pp-process produces an equal number of pions of all three charges and that the neutral pion decays into two gamma-ray photons for every charged pion producing a muon neutrino and antineutrino pair. For a power-law spectrum with a power-law index Γ, the relation of gamma-ray flux to neutrino flux is a simple factor of $2^{1-\Gamma}$ (e.g. Ahlers & Halzen 2018, their equation 3). We then estimated the number of neutrinos detected by IceCube with the following:

$$N_\nu = \int A_{\rm eff}(E) F_\nu(E) {\rm d}E {\rm d}t, \quad (3)$$

where $A_{\rm eff}(E)$ is the IceCube effective area at the declination of Cyg X-3 (41 deg) for appropriate observing seasons provided in the 10-yr event sample and $F_\nu(E)$ is the incident neutrino flux. The integration goes through the times of the HE gamma-ray flaring periods and neutrino energies 1–50 TeV. The total accumulated gamma-ray flaring period length is 354 d during the IceCube seasons from 2008 to 2018. The estimated average number of detected >1 TeV neutrinos during the flaring states is 1.0. Thus, the probability of observing more than one neutrino with this average is 27 per cent for Poisson-distributed events.

In addition, using the upper limit on the time-integrated neutrino flux from Cyg X-3 derived in Abbasi et al. (2022) ($dN/dE = 8.6\,(E/{\rm TeV})^{-2.5} \times 10^{-12}\,{\rm TeV}^{-1}\,{\rm cm}^{-2}\,{\rm s}^{-1}$) and assuming that all the neutrino emission takes place in the HE gamma-ray flaring periods, which then allows for a ten times higher flux, results in a maximum of 3–4 neutrinos with soft 2–3 TeV energies. Therefore, in our scenario, we are well within the upper limits derived in Abbasi et al. (2022).

4.2 The HE gamma-ray association to Cyg X-3

The HE gamma-ray field of Cyg X-3 is complex due to nearby star formation sites, OB associations, and gamma-ray pulsars (Tavani et al. 2009; Zdziarski et al. 2018). Therefore, it is unclear whether the low-level HE gamma-ray flux can be attributed solely to Cyg X-3. In Fig. 2, we delineated the phases of HE gamma-ray flares to those that rise above one standard deviation from the mean level ($>0.6 \times 10^{-6}$ photons s^{-1} cm^{-2} or $>3 \times 10^{-10}$ erg s^{-1} cm^{-2} in the 0.1–100 GeV band). These flaring events can be unequivocally attributed to Cyg X-3 due to their temporal occurrence with the phases of low flux of the hard X-ray emission (Fig. 2) as well as presenting clear modulation when folded to the 4.8-h binary orbit (Fermi LAT Collaboration 2009; Zdziarski et al. 2018). This modulation has a maximum at phase 0.8, close to the superior conjunction of the binary orbit. Therefore, the probability of receiving a neutrino close to phase 0.8 is greater (as in the case of the event at MJD 55600). However, we note that the HE gamma-rays are emitted during all orbital phases (Prokhorov & Moraghan 2022).

4.3 Contribution to the cosmic ray sea

The origin of Galactic cosmic rays is still an open question (see e.g. a recent review by Gabici et al. 2019). Supernova remnants are regarded as promising sources of Galactic cosmic rays with energies up to 10^{15} eV – the 'knee' of the cosmic ray spectrum (see e.g. Ackermann et al. 2013; Cao et al. 2021a). Over the last decade, space- and ground-based telescopes have revealed several new classes of Galactic gamma-ray source populations, some of which could also contribute to Galactic cosmic rays. These include for example pulsar wind nebulae (e.g. H. E. S. S. Collaboration 2018), stellar clusters (e.g. Cygnus cocoon; Ackermann et al. 2011; Abeysekara et al. 2021), and massive stars (e.g. Aharonian, Yang & de Oña Wilhelmi 2019). The list also includes XRBs, which were already suggested as potential sources of cosmic rays at the beginning of the century (Heinz & Sunyaev 2002; Fender, Maccarone & van Kesteren 2005). While leptonic processes can partially explain the HE gamma-ray emission, neutrino detection directly implies that hadrons are accelerated to GeV−TeV energies in Cyg X-3. This implies that Cyg X-3 could contribute to its local pool of cosmic ray sea. However, due to its rare nature (we expect one black hole Wolf–Rayet binary at a given time in our Galaxy; Lommen et al. 2005), the contribution at the Galaxy level is vanishingly small.

[1] https://github.com/icecube/PSLab_PS_analysis

The amount of energy contained in the protons ejected in the jet of Cyg X-3 can be estimated as $E_p = L_p t_p \approx 1.7 \times 10^{40}$ erg, where $L_p = 10^{38}$ erg s^{-1} and the proton confinement time $t_p = 0.01 \times 4.8$ h (Sahakyan et al. 2014). As the active HE gamma-ray flaring duty cycle during the 10-yr IceCube observations is approximately 10 per cent (354 d in 10 yr), the total energy rate is $\sim 10^{39}$ erg yr^{-1}.

5 CONCLUSIONS

The spatial and temporal association of neutrino emission from Cyg X-3 during HE gamma-ray flaring states has important implications, providing evidence for a new class of astrophysical neutrino emitters and showing that protons are accelerated to high energies in Cyg X-3's jet during these states. This has implications for the origin of Galactic cosmic rays and the hadron content of jets.

Microquasars and radio-loud quasars have been debated as potential sources of hadronic acceleration for decades. Given the similarity of the two systems (Merloni, Heinz & di Matteo 2003; Liodakis et al. 2017), the recent potential association of blazars with high-energy ∼PeV neutrinos (IceCube Collaboration 2018) makes the scenario of lower-energy neutrinos coming from microquasars plausible. The hadron loading of the jet in microquasars can occur through the accretion of large-scale magnetic fields that mix disc matter with the jet (McKinney & Blandford 2009; Cao et al. 2021b) or entrainment of protons from the companion star's stellar wind (e.g. Romero et al. 2003), both of which have a high probability of occurring in Cyg X-3 due to the short orbital separation and dense stellar wind.

The multiwavelength evolution and neutrino emission in Cyg X-3 strengthen the scenario in which the jet interacts with the dense stellar wind of the Wolf–Rayet companion. This interaction is further enhanced in the soft state when the jet is switched off and the missing ram pressure causes the wind to fill the cavity blown by the jet. As the jet begins to form again, it encounters a far denser medium than during the hard state, leading to efficient shock formation and energy dissipation through radio, gamma-ray, and neutrino emission. The recent higher duty cycle of the soft state in Cyg X-3 and corresponding times of HE gamma-ray emission may lead to more than double the neutrino detections from Cyg X-3 in upcoming IceCube data releases.

ACKNOWLEDGEMENTS

This project has received funding from the European Research Council (ERC) under the European Union's Horizon 2020 research and innovation programme (grant agreement no. 101002352). KS and EJL were supported by the Academy of Finland projects 317636 and 320045.

DATA AVAILABILITY

The all-sky point-source muon track data set from the IceCube Neutrino Observatory gathered between 2008 and 2018 is publicly available at http://doi.org/DOI:10.21234/sxvs-mt83. The *Fermi*-LAT weekly light curve of Cyg X-3 can be found at https://fermi.gsfc.nasa.gov/ssc/data/access/lat/LightCurveRepository/source.php?source_name=4FGL_J2032.6+4053#. The *Swift*/BAT daily light curve of Cyg X-3 can be found at https://swift.gsfc.nasa.gov/results/transients/CygX-3/.

REFERENCES

Aartsen M. G. et al. 2017, J. Instrum., 12, P03012
Abbasi R. et al., 2022, ApJ, 930, L24
Abdollahi S. et al., 2023, preprint (arXiv:2301.01607)
Abeysekara A. U. et al., 2021, Nat. Astron., 5, 465
Ackermann M. et al., 2011, Science, 334, 1103
Ackermann M. et al., 2013, Science, 339, 807
Aharonian F., Yang R., de Oña Wilhelmi E., 2019, Nat. Astron., 3, 561
Ahlers M., Halzen F., 2018, Prog. Part. Nucl. Phys., 102, 73
Aleksić J. et al., 2010, ApJ, 721, 843
Antokhin I. I., Cherepashchuk A. M., 2019, ApJ, 871, 244
Archambault S. et al., 2013, ApJ, 779, 150
Baerwald P., Guetta D., 2013, ApJ, 773, 159
Bulgarelli A. et al., 2012, A&A, 538, A63
Cao Z. et al., 2021a, Nature, 594, 33
Cao Z. et al., 2021b, Nature, 594, 33
Corbel S. et al., 2012, MNRAS, 421, 2947
Dubus G., Cerutti B., Henri G., 2010, MNRAS, 404, L55
Fender R. et al., 1999, ApJ, 519, L165
Fender R. P., Belloni T. M., Gallo E., 2004, MNRAS, 355, 1105
Fender R. P., Maccarone T. J., van Kesteren Z., 2005, MNRAS, 360, 1085
Fermi LAT Collaboration, 2009, Science, 326, 1512
Gabici S., Evoli C., Gaggero D., Lipari P., Mertsch P., Orlando E., Strong A., Vittino A., 2019, Int. J. Mod. Phys. D, 28, 1930022
Giacconi R., Gorenstein P., Gursky H., Waters J. R., 1967, ApJ, 148, L119
H. E. S. S. Collaboration, 2018, A&A, 612, A1
Heinz S., Sunyaev R., 2002, A&A, 390, 751
IceCube Collaboration, 2013, ApJ, 763, 33
IceCube Collaboration, 2018, Science, 361, eaat1378
IceCube Collaboration, 2021, All-sky point-source IceCube data: years 2008-2018. Dataset
Kelner S. R., Aharonian F. A., Bugayov V. V., 2006, Phys. Rev. D, 74, 034018
Koljonen K. I. I., Hannikainen D. C., McCollough M. L., Pooley G. G., Trushkin S. A., 2010, MNRAS, 406, 307
Koljonen K. I. I., Maccarone T. J., 2017, MNRAS, 472, 2181
Koljonen K. I. I., Maccarone T., McCollough M. L., Gurwell M., Trushkin S. A., Pooley G. G., Piano G., Tavani M., 2018, A&A, 612, A27
Krimm H. A. et al., 2013, ApJSS, 209, 14
Liodakis I. et al., 2017, ApJ, 851, 144
Lommen D., Yungelson L., van den Heuvel E., Nelemans G., Portegies Zwart S., 2005, A&A, 443, 231
McKinney J. C., Blandford R. D., 2009, MNRAS, 394, L126
Merloni A., Heinz S., di Matteo T., 2003, MNRAS, 345, 1057
Parsignault D. R. et al., 1972, Nat. Phys. Sci., 239, 123
Piano G. et al., 2012, A&A, 545, A110
Prokhorov D. A., Moraghan A., 2022, MNRAS, 519, 2680
Romero G. E., Torres D. F., Kaufman Bernadó M. M., Mirabel I. F., 2003, A&A, 410, L1
Sahakyan N., Piano G., Tavani M., 2014, ApJ, 780, 29
Tavani M. et al., 2009, Nature, 462, 620
van Kerkwijk M. H. et al., 1992, Nature, 355, 703
Zdziarski A. A. et al., 2018, MNRAS, 479, 4399
Zdziarski A. A., Sikora M., Dubus G., Yuan F., Cerutti B., Ogorzałek A., 2012, MNRAS, 421, 2956

This paper has been typeset from a TEX/LATEX file prepared by the author.